

Document downloaded from:

<http://hdl.handle.net/10251/101668>

This paper must be cited as:



The final publication is available at

<http://doi.org/10.1021/jp805400u>

Copyright American Chemical Society

Additional Information

This document is the Accepted Manuscript version of a Published Work that appeared in final form in

The Journal of Physical Chemistry C, copyright © American Chemical Society after peer review and technical editing by the publisher.

To access the final edited and published work see <http://doi.org/10.1021/jp805400u>

Published Work, see <http://pubs.acs.org/page/policy/articlesonrequest/index.html>

Synthesis of Ti-silicate form of BEC polymorph of Beta zeolite assisted by molecular modeling

*Manuel Moliner, Pedro Serna, Ángel Cantín, Germán Sastre, María J. Díaz-Cabañas, Avelino Corma**

Instituto de Tecnología Química (UPV-CSIC), Av. Naranjos s/n, E-46022 Valencia, Spain.

e-mail: acorma@itq.upv.es

RECEIVED DATE (to be automatically inserted after your manuscript is accepted if required according to the journal that you are submitting your paper to)

ABSTRACT. The K^+ free pure silica form of polymorph C (BEC) of Beta zeolite has been synthesized with a cationic organic structure directing agent (SDA) that was predicted best, out of a series of nine potentials, by means of modeling techniques. On the bases of this synthesis method, the Ti-BEC zeolite has been obtained which owing to the pore topology and dimensions shows a higher epoxidation activity than the Ti-Beta polymorph either with H_2O_2 or organic peroxides as oxidants.

KEYWORDS. Zeolite synthesis, polymorph, structure directing agent, molecular modeling, epoxidation.

1.- INTRODUCTION.

The introduction of well defined single catalytic sites in the walls of molecular sieves allows preparing highly selective catalysts in where diffusion, adsorption and reactivity could be tailored in many cases to achieve optimum results.¹ In this way, microporous and mesoporous molecular sieves catalysts containing different framework transition metal atoms and transition metal complexes have been successfully prepared.²

In the case of titanosilicates and since the discovery of TS-1,³ researchers have tried to introduce Ti species into the framework of alternative structures in order to improve activity, selectivity and reactant accessibility for manufacturing oxygenated derivatives. More specifically, epoxidation reactions have attracted a great interest owing to the facility of the oxirane group to be transformed into other important intermediates. TS-1, being so far the best Ti-silicate epoxidation catalyst for smaller olefins when using as oxidant H₂O₂, becomes limited when large size olefins or organic peroxides are to be reacted. In those cases, the use of large pore zeolites and structured mesoporous silicates containing Ti in the framework, have opened new opportunities. Ti-Beta was the first large pore Ti zeolite synthesized that showed selective epoxidation of olefins, with either H₂O₂ or organic peroxides,⁴ and has been used as a landmark for comparing the catalytic behavior of Ti-large pore zeolites. Recently, Tatsumi et al. reported a new interesting titanosilicate molecular sieve, Ti-YNU-1,⁵ with high activity and selectivity in the epoxidation of cycloalkenes with H₂O₂. This expanded structure of the MWW zeolite showed high turnovers when reacting cycloalkenes up to seven carbons, while a notable decrease in activity was observed for larger substrates. The authors presented that Ti-Beta gives a lower activity than Ti-YNU-1 for cycloalkene rings with seven or less members, but their activity becomes closer for the epoxidation of cyclooctene.

It appeared to us that the catalytic behavior of Ti-Beta could be improved if one was able to synthesize a Ti-silicate form of the polymorph C of Beta. Indeed, this polymorph with a three-dimensional arrange of large straight channels (7.5x6.3 Å and 6.9x6.0 Å), instead of the two straight 6.6x6.7 Å and one

sinusoidal $5.6 \times 5.6 \text{ \AA}$ of Beta,⁶ should allow larger molecules to diffuse within the pores with the corresponding increase in activity. Unfortunately, Al-free polymorph C of Beta (BEC) was only obtained as a germanate⁷ or as a silico-germanate,⁸ and the Ti form of the second one gave, in our hands, low activity. Recently, it has been presented a new synthetic route for obtaining the pure silica polymorph C of Beta zeolite, working in a buffered media with hexafluorosilicate species and K^+ cations, using as Structure Directing Agent (SDA) SDA1 given in Figure 1.⁹ While the pure silica polymorph C opens the possibility to synthesize the Ti-silicate form, the presence of K^+ in the synthesis precludes this possibility due to the precipitation of potassium titanates during the synthesis process.¹⁰ Therefore, if a Ti-BEC zeolite wants to be obtained, it is necessary first to find a SDA and a new procedure for the synthesis of the pure silica BEC polymorph in an alkaline free medium. If this would be achieved, then the synthesis of the Ti-silicate could be attempted.

In this paper, we will show that by modeling techniques it was possible to predict that two out of nine potential organic SDAs can better stabilize the pure silica form of polymorph C. Then, with one of these two SDA we have achieved the K^+ free synthesis of pure silica BEC and Ti-BEC. This zeolite shows, as predicted, a better catalytic behavior than Ti-Beta or any other previously reported zeolite for epoxidation of cycloalkenes.

2.- EXPERIMENTAL

2.1.- COMPUTATIONAL METHODS

The calculations have been performed using lattice energy minimization techniques^{11,12} and the GULP code,¹³ employing the Ewald method for summation of the long range Coulombic interactions, and direct summation of the short range interactions with a cut off distance of 12 \AA . The RFO (rational functional optimizer) technique was used as the cell minimization scheme with a convergence criterion of a gradient norm below 0.001 eV/\AA . Full optimizations of all the atoms of the system (zeolite + SDA) have been performed, and also the unit cell parameters were optimized. A semiempirical shell model forcefield for Si/F zeolites^{14,15} has been used throughout. To account for the effect of the SDA in the

system, the forcefields by Kiselev et al.,¹⁶ and by Oie et al.¹⁷ have been used for the intermolecular SDA zeolite and intra and intermolecular SDA interactions. For the SDA, the charge distribution has been obtained by means of the Charge equilibration method.¹⁸ The 9 SDAs used in the simulations are shown in Figure 1.

Another important aspect in our methodology is the treatment of the total energy and the different terms that influence the total energy. Some previous studies taking into account the thermodynamic aspects of the synthesis of zeolites as well as a rough estimation of some aspects related to the kinetics have been presented.¹⁹ From that approach an approximation to the energy change of the system upon SDA incorporation is:

$$\Delta E = E_{f, i} - E_{i, i} - n \cdot E_{z, i} + \frac{1}{N} \sum_i^n (E_{s, i} - E_{s, 0}) + \frac{1}{N} \sum_i^n E_{z, i} \quad (1)$$

In this equation, the notation 'zeo' and 'sda' refer to the geometry of the final system where both the zeolite and the template are more or less far from the optimized ground state conformations. It is noted that if the synthesis is viable this will be reflected in the fact that the energetic penalty will be low due to the matching between zeolite and SDA, which precisely justifies the use of SDAs in the synthesis of zeolites. The energies are per TO₂ unit and the number of them in the unit cell of choice for the calculations is called N, thus we divide by N where appropriated, whereas the energy of the zeolite is always defined per TO₂ unit and can be referred with respect to the energy of quartz. In the same equation, n is the number of templates fitted in the corresponding unit cell. The energy expression above contains the four more important energetic factors controlling the synthesis of zeolites in fluoride media from the thermodynamic viewpoint:

- (i) Stable zeolite structures (low E_{zeo'}) will be favored.
- (ii) Occluded SDA molecules should have energy close to the ground energy, so as to minimize

ΔE_{SDA} .

(iii) High attractive intermolecular interactions between the zeolite and the SDA_t will favor the synthesis. This leads to a close matching between the sizes and shapes of the SDA molecular surface and the zeolite microporous void.

(iv) Electrostatic orderings that minimize the energetics of SDA-F location are favored (this includes SDA⁺-SDA⁺, SDA⁺-F⁻, and F⁻-F⁻).

GULP full optimizations proceed by taking into account the total energy of the system (zeo+SDA) until a global minimum is reached and this is the final state of the system. When the minimum is obtained, the corresponding configuration is taken to calculate the terms in the equation (1) above.

2.2.- SYNTHESIS OF SDAs

The structure directing agents synthesized in this work are shown in Figure 1. The synthesis procedure was as follows:

- Synthesis SDA1, SDA2, SDA3, and SDA4

The starting materials for the synthesis of SDA-1, -2, -3, and -4 were *1,3-cyclohexadiene* and *N-methylmaleimide*, *cycloheptatriene* and *N-methylmaleimide*, *cyclopentadiene* freshly distilled from dicyclopentadiene and *N-methylmaleimide*, and *cyclopentadiene* freshly distilled from dicyclopentadiene and *maleimide*, respectively.

Synthesis of Diels-Alder adducts: A toluene solution (350 mL) of the corresponding diene (103 mmol) and maleimide or N-methylmaleimide (103 mmol) was refluxed for 4 days. After cooling, the resulting precipitate was filtered and washed with hexane to give the Diels-Alder product in quantitative form.

Reduction of the Diels-Alder adducts. The Diels-Alder adduct (51 mmol) was slowly added to a suspension of LiAlH₄ (127 mmol) in anhydrous diethyl ether or THF (250 mL) at 0°C under N₂ atmosphere. When the addition was completed the mixture was refluxed for 5 hours and stirred at room temperature overnight. The reaction was quenched by addition of H₂O (10 mL), 15% aqueous solution of NaOH (10 mL) and distilled H₂O (10 mL). After 30 min stirring at room temperature the solution was

filtered and extracted with diethyl ether. The combined organic extracts were washed with brine, dried and concentrated to dryness providing the corresponding reduced product (89%).

Alkylation of tertiary amines. CH_3I (1.7 mol) was added to a solution of the tertiary amine (33.5 mmol) in diethyl ether (85 mL). The mixture was stirred 7 days at room temperature and the precipitate formed was washed with diethyl ether providing quantitatively the desired quaternary salt.

Alkylation of secondary amines with 1,4-dibromobutane (SDA4). The secondary amine (45 mmol) was added dropwise at 100°C to a suspension of 1,4-dibromobutane (45 mmol) in a 1.5 M solution of NaOH. The mixture was stirred for 3 hours, was poured into a 40% NaOH solution and extracted with CH_2Cl_2 . The combined organic extracts were dried over MgSO_4 and concentrated to dryness yielding the corresponding reduced product (65%).

- *Synthesis SDA5, and SDA6*

The starting reactants for the synthesis of SDA-5, and -6 were *N*-methyl-2-pyridone and *N*-methylmaleimide, and 1,3-dimethyl-2-pyridone and *N*-methylmaleimide, respectively. 1,3-dimethyl-2-pyridone was prepared as follows:²⁰ A suspension of arecoline hydrochloride (0.026 mol) in *n*-butyl alcohol (50 mL) was treated with potassium tert-butoxide (0.053 mol) and stirred at reflux under argon for 48 h. The cooled mixture was treated with concentrated hydrochloric acid (2 mL) and stirred overnight. The resulting suspension was diluted with ether (150 mL) and filtered. The filter cake was washed with ether (50 mL). The combined filtrate and wash was stripped of solvent on a rotary evaporator using a 70°C bath and water aspirator vacuum. The pale yellow liquid residue was 1,3-dimethyl-2-pyridone (0.022 mol, 86% yield).

Synthesis of Diels-Alder adducts. A toluene solution (250 mL) of the corresponding diene (103 mmol) and *N*-methylmaleimide (103 mmol) was refluxed for 5 days. After cooling, the solvent was eliminated in the rotary evaporator providing the desired imidolactones (75%).

Reduction of the imidolactones. To a suspension of LiAlH_4 (298 mmol) in anhydrous THF (250 mL) was slowly added the corresponding imidolactone (60 mmol) under N_2 and at 0°C . When the addition was finished the mixture was refluxed for 5 hours and stirred at room temperature overnight. Then, the

reaction was quenched by addition of H₂O (10 mL), 15% aqueous solution of NaOH (10 mL) and distilled H₂O (10 mL). After 30 min stirring at room temperature the solution was filtered, partially concentrated and then extracted with dichloromethane. The combined organic extracts were washed with brine, dried and concentrated to dryness providing the corresponding reduced product (75%).

Alkylation of diamines. To a solution of the diamine (33.5 mmol) in methanol (85 mL) was added CH₃I (1.7 mol). The mixture was stirred 7 days at room temperature. The mixture is concentrated in vacuo obtaining the desired diamonium salt (79%).

- *Synthesis SDA7, and SDA8*

The starting materials for the synthesis of SDA-7, and -8, were *bicyclo[2.2.1]oct-7ene-2,3,5,6-tetracarboxylic dianhydride*, and *4,6-dimethyl- α -pyrone* and *maleic anhydride*, respectively.

Synthesis of Diels-Alder adduct from 4,6-Dimethyl- α -pyrone and maleic anhydride. A toluene solution (500 mL) of 4,6-Dimethyl- α -pyrone (161 mmol) and maleic anhydride (322 mmol) was refluxed for 5 days. After cooling, the resulting precipitate was filtered and washed with hexane to give the corresponding bicyclodianhydride (87%).

Amination of bicyclodianhydrides. Bicyclodianhydride products (140 mmol) were solved in ethylamine solution (70% in H₂O) (400 mL) and refluxed for 3.5 days. After cooling, the solvent was eliminated in the rotary evaporator providing the desired diimides in quantitative form.

Reduction of diimides. To a suspension of LiAlH₄ (244 mmol) in anhydrous THF (300 mL) was slowly added the corresponding diimide (49 mmol) under N₂ and at 0° C. When the addition was finished the mixture was refluxed for 5 hours and stirred at room temperature overnight. Then, the reaction was quenched by addition of H₂O (10 mL), 15% aqueous solution of NaOH (10 mL) and distilled H₂O (10 mL). After 30 min stirring at room temperature the solution was filtered, partially concentrated in the rotary evaporator and then extracted with dichloromethane. The combined organic extracts were washed with brine, dried and concentrated to dryness providing the corresponding amines (66%).

Alkylation of the diamine. Iodomethane (642 mmol) was added over a solution of diamine (52 mmol) in 70 ml of methanol. The mixture was stirred at room temperature for 72 hours and after that a new addition of the same amount of methyl iodide was added and kept under stirring 72 hours. Then, the final organic dication was concentrated under vacuum and precipitated by addition of diethyl ether. The precipitate was filtered under vacuum yielding to 20.8 g (89%) of the diquaternary ammonium as diiodide salt

- *Synthesis SDA9*

The starting materials for the synthesis of **SDA9** were *N-methylmaleimide* and *bencene*.

Cycloaddition of *N-methylmaleimide* and *bencene*. A solution of *N-methylmaleimide* (108 mmol) in a mixture of *bencene* (300 mL), acetophenone (30 mL) and acetone (84 mL) was distributed in 10 Pyrex tubes. Prior to the photochemical reaction, N₂ was flowed through the solutions for 15 minutes and, afterwards, were irradiated under stirring with a high pressure Hg lamp (200< λ <90 nm) during 48 hours. The resulting precipitate was filtered under vacuum providing the desired diimide (40 %).

Reduction of the diimide. To a suspension of LiAlH₄ (244 mmol) in anhydrous THF (300 mL) was slowly added the corresponding diimide (49 mmol) under N₂ and at 0° C. When the addition was finished the mixture was refluxed for 5 hours and stirred at room temperature overnight. Then, the reaction was quenched by addition of H₂O (10 mL), 15% aqueous solution of NaOH (10 mL) and distilled H₂O (10 mL). After 30 min stirring at room temperature the solution was filtered, partially concentrated in the rotary evaporator and then extracted with dichloromethane. The combined organic extracts were washed with brine, dried and concentrated to dryness providing the corresponding diamine (70%).

Alkylation of the diamine. To a solution of the diamine (33.5 mmol) in methanol (85 mL) was added CH₃I (1.7 mol). The mixture was stirred 7 days at room temperature. The mixture is concentrated under vacuum obtaining the desired diamonium salt (75%).

2.3.- SYNTHESIS OF ZEOLITES

- *Synthesis of pure silica materials*

A typical synthesis was as follows: the SDA hydroxide was mixed with the required quantity of Ludox AS-40 and a solution of NH₄F (10%wt). Then the mixture was stirred until evaporation of the excess of water.

The final gel composition was fixed as:



The gels were heated at 175°C in Teflon lined stainless steel autoclaves for 14 days, and after this, the solids were filtered, washed and dried at 100°C.

- *Synthesis of silicotitanate Ti-BEC (Ti-ITQ-17)*

A typical Ti-ITQ-17 synthesis is as follows: 1.411 g of the SDA9 hydroxide solution (16% wt.) was mixed with 0.451 g of Ludox AS-40 and 0.010 g of titanium ethoxide (Alfa Aesar). Then, 0.555 g of NH₄F solution (10% wt.) was added to the gel, and the mixture was stirred until evaporation of the excess of water. Finally, 0.012 g of ITQ-17 crystals seeds were added.

The final composition of the gel was:



The gel was heated at 175°C in Teflon lined stainless steel autoclaves for 14 days, and the resultant solid was filtered, washed and dried at 100°C.

2.4.- CATALYTIC TESTS

Reactions were carried out in 2-ml glass flasks with magnetic stirring and heated by means of a temperature controlled aluminum rack. Catalytic tests by using H₂O₂ as oxidant were performed at 333 K, using 10 mgr of catalyst per mL of a reaction mixture with the following molar composition: 93.3 % acetonitrile, 5.3 % olefin, and 1.4 % H₂O₂ (from commercial reactants). On the contrary, experiments with *tert*-butyl hydroperoxide (TBHP) as oxidant were carried out under solvent-free conditions, using

15 mgr of catalyst per mL of a reaction mixture with an olefin/oxidant molar ratio equal to 4:1. All substances were available from *Sigma-Aldrich Company* (Acetonitrile, 99 %; 1-hexene, 99 %; cyclohexene, 99 %; *cis*-cyclooctene, 95 %; cyclododecene, 99 %; H₂O₂, 35 wt % in water; TBPH, 80 % in a mixture di-*tert*-butylperoxide/water 3/2). Aliquots were automatically taken with an autosampler (Konic K-MAS5), and analyzed on-line by gas chromatography. Calculations of conversion and selectivity levels were done according to corrected chromatographic areas, while products were identified by comparing their GC-MS spectra with the corresponding pure commercial substances.

2.5.- CHARACTERIZATION

XRD measurements:

X-ray powder diffraction data were collected using a multi-sample Phillips X'Pert diffractometer with Bragg-Brentano geometry. Intensity data were obtained with a variable divergence slit using the CuK α 1,2 radiation.

Solid state NMR:

NMR spectra were recorded at room temperature under magic angle spinning (MAS) in a Bruker AV-400 spectrometer. NMR¹⁹F was measured at 376.28 MHz using a Bruker probe with 2.5 mm diameter zirconia rotors spinning at 25 kHz. The ¹⁹F spectra were collected using pulses of 4.5 μ s corresponding to a flip angle of $\pi/2$ rad, and a recycle delay of 100 s to ensure the complete recovery of the magnetization. The single pulse ²⁹Si spectra were acquired at 79.5 MHz with a 7 mm Bruker BL-7 probe using pulses of 3.5 μ s corresponding to a flip angle of $3/4 \pi$ radians, and a recycle delay of 60 s.

Chemical analysis (C, N, H) was carried out by combustion using a Perkin-Elmer analyzer and titanium and silicon contents were determined with a Varian ICP. A Cary 5 spectrometer equipped with a diffuse reflectance accessory was used for UV measurements.

3.- RESULTS AND DISCUSSION

3.1.- SDA selection and theoretical calculations

As we said before, SDA-1 was able to direct the synthesis towards the all silica form of BEC in the presence of K. Therefore, we thought first on various monocationic SDAs of the same family in where the core structure of the SDA1 (*4,4-dimethyl-4-azonia-tricyclo[5.2.2.0^{2,6}]undec-8-ene*) was maintained.

A second series of SDA (SDA-5 and -6) with similar molecular size than SDA1-4 but with two charges in the structure, have also been considered for the synthesis of BEC. Finally, in a third option, larger and more rigid dicationic SDAs (SDA7-9) have been thought as potential organics. At this point, we decided to study the possibility of predicting which can be the most adequate SDA by means of computational methods directed to find the SDA that better minimizes the energy of the self assembled system all silica BEC-SDA.

Monocationic SDAs.

The monocationic SDAs in Figure 1 present conformational isomerism endo-exo according to the position of the substituents in the carbon atoms belonging to rings. Initially some conformations are more feasible than others taking into account the Diels-Alder reaction from which the SDA is synthesized but, nevertheless, thermal interconversion between isomers might be possible if the activation energy required is sufficiently low. For this reason we have calculated all the isomers and we have taken the most stable configuration for modeling.

A BEC unit cell, contains 32 Si atoms and two D4Rs (double four rings) which are filled with one fluorine anion. An optimal loading of 2 SDA molecules has been found optimum in all cases. With the monocationic SDAs (SDA1-SDA4) this means a neutral system. Therefore, two molecules of SDA and two fluoride anions have been located in the unit cell (32 SiO₂) of pure silica BEC zeolite. Two D4R cages are available in the unit cell and this makes easy the fluoride location, since only one configuration is possible, with one fluoride in each D4R. Regarding the SDA loading, several concentrations were tested giving an optimum of two molecules per unit cell. The two SDA cations are located randomly in the microporous space and several initial orientations have been tested in order to

explore, as completely as possible, the different orientation opportunities in search for the global minimum. We remark that during the optimization (search of the geometry with minimum energy), all the atoms of the system are allowed to relax without any symmetry constraints, and also the cell parameters were optimized without symmetry constraints.

From the final geometry, the energetic contributions shown in Table 1 are calculated. For the monocationic SDAs (SDA1-SDA4), three energetic terms are directing the synthesis. Two of them are the short-range (van der Waals) interaction zeolite-SDA ($E^{\text{vdW}}_{\text{zeo-SDA}}$), and the long-range (electrostatic) interactions between charged particles ($\text{SDA}^+-\text{SDA}^+$, SDA^+-F^- , and F^--F^- , called $E^{\text{coul}}_{\text{SDA,F}}$). Synthesis products are more favorable when the lower the energy of any (or both) of these two terms is. The third energetic term invoked to explain the synthesis results is the SDA strain (ΔE_{SDA}), which controls the synthesis results in a different way: high values of ΔE_{SDA} *preclude* the synthesis, whilst low values of ΔE_{SDA} *do not preclude* the synthesis. The different contributions (Table 1) show that SDA1 and SDA4 are the most favorable. From the point of view of the $E^{\text{coul}}_{\text{SDA,F}}$, SDA1 is the most favorable with an energy of -6.40 eV (Table 1), which indicates a very favorable charge distribution, due to close distances between opposite charge ions, SDA-F, and large distances between equal charge ions, SDA-SDA. Favorable electrostatic SDA,F contributions are believed to play a significant role during the nucleation stage and, from the computational viewpoint, this is a reason to consider SDA1 as a good candidate for the synthesis of pure silica BEC.

Dicationic SDAs.

When the same methodology for calculations has been applied to the dicationic OSDAs, we face the problem that the F^- present in the two D4R can not compensate the four positive charges of the two template molecules, and the energetics of dicationic species has leaded us to consider the role of framework-defects as a part of the BEC structure. In a defect, a Si atom disappears and creates 4 unsaturated terminals Si-O^- bonds. Three of these bonds are then saturated by protons and hence, overall, the internal framework defect appears as one unsaturated Si-O^- bond and three terminal SiOH

bonds (see Figure 2). The overall charge of the defect is -1. Two defects and two fluorine anions, together with the two dicationic SDA molecules make a neutral framework which can be considered as generated from: $30\text{SiO}_2 + 2\text{H}_2\text{O} + 2\text{OH}^- + 2\text{F}^- + 2\text{SDA}^{2+}$.

From the computational viewpoint, we have used the forcefield by Catlow et al.²¹ which was parameterized to treat in a realistic way hydroxyl groups in zeolites. Our test calculations show that the optimization of the previously described defects gives reasonable geometries and therefore we consider this as a reasonably accurate approximation. For the sake of further accuracy we were considered several framework-defect orientations. Whilst fluorine anions are well localized in the framework, many possibilities for defect locations can be considered and consequently instead of considering only one possibility, we have calculated 5 different configurations of two defects in the unit cell. In each case the unit cell parameters and all the atoms of the structure have been fully reoptimized to find the minimum energy configuration. From the corresponding final geometries, the total energy was calculated, excluding the internal SDA energy whose stress was already considered previously. The results (Table 3) indicate the relative energies of the framework-defect configurations. It can be seen that, taken together, the results corresponding to SDA9 give the minimum energy and hence the maximum stability. The corresponding average values are 1.29, 1.21, 1.65 and 0.96 eV for SDA5, SDA6, SDA7 and SDA9 respectively. For the sake of comparison with monocationic SDAs we have also calculated van der Waals energies and SDA stress energies for the dicationic SDAs, and the details of the calculations are given in the supplementary material. SDA stress energies give favorable values for SDA9, and also the short range van der Waals energy was favorable for SDA9 (Table 2). In conclusion, the calculations introducing the framework defects strongly support SDA9 as a good candidate for the synthesis of pure silica BEC zeolite. Further, the excellent fit (coming from the high stabilisation short range van der Waals energy in Table 2) between the SDA9 and the BEC structure can be visualised from Figure 3.

3.2.- Zeolite synthesis and characterization

In the selected synthesis conditions (see experimental section), it was found that SDA1, which leads to the pure silica form of polymorph C in the presence of K^+ and high pH, yields Beta zeolite under K^+ -free and neutral pH (see Table 4). In the same way, other small monocationic SDAs belonging to the same family (SDA2, SDA3, and SDA 4) also produce Beta structure. Dicationic SDA5 and SDA6, with similar sizes than SDA1 to SDA4 but with two charges in their structure always yield amorphous materials under the same synthesis conditions. On the other hand when SDA7-9 with larger and more rigid dicationic molecular structures were used as SDA, it was found that SDA9, which is twice larger than SDA1 but presenting two charges, leads to the formation of a highly crystalline polymorph C under K-free conditions (see X-Ray diffractogram in Figure 4), while SDA7 and SDA8 yield Beta and ITQ-24 zeolite, respectively.

The ^{19}F NMR spectrum of as made ITQ-17 with SDA9 (see Figure 5) confirms that only the characteristic peak of the D4R signal is observed at -38 ppm. The chemical analysis of the as synthesized ITQ-17 (see Table 5) indicates the presence of two molecules per unit cell as was considered with the molecular calculation. In these conditions, fluoride anions inside D4R (2 D4R/u.c.) are not balancing the excess of positives charges coming from the SDA molecules, and thus structural defects are expected in this zeolite, as it is shown in the ^{29}Si NMR spectrum of the as made ITQ-17 sample obtained with SDA9 (see Figure 6). Indeed, the band at -100 ppm, assigned to Si_3OH species in the zeolite, is clearly more intense in the case of SDA9 than SDA1, indicating that a higher amount of connectivity defects are present in the framework of this material in agreement with the postulates made for theoretical calculations. The excellent fitting of SDA9 within the void space of BEC structure makes this organic molecule a very selective directing agent to synthesize the pure silica BEC structure.

Interestingly, the procedure described here does not require the presence of alkali cations during the synthesis process, opening the door for the introduction of framework Ti species. Thus, taking into account the potential catalytic interest of Ti-ITQ-17, we have carried out the synthesis of this material with SDA9 as organic structure directing agent (see experimental section and Table 6). A Ti-ITQ-17 material with high crystallinity has been obtained, and the UV-Vis diffuse reflectance spectrum of the

calcined sample shows the presence of a unique band at ~ 220 nm, which can be assigned to Ti tetrahedrally coordinated into the zeolite framework (Figure 7).²²

3.3.- Catalytic results

The catalytic behavior of Ti-Beta and Ti-ITQ-17 was evaluated for the epoxidation of cyclic and non cyclic olefins with H₂O₂ as oxidizing agent. The intrinsic activity of these catalysts is given as a turnover frequency number (mmol alkene converted/mmol Ti.h), calculated from initial reaction rates (see Figure 8). Despite the higher intrinsic chemical reactivity of cyclic than linear terminal olefins for epoxidation, Ti-Beta gives similar activity when reacting 1-hexene, cyclohexene and cyclooctene, while a sharp decrease in activity is produced for the largest substrate, cyclododecene. The low epoxidation rate for the C₁₂ olefinic can be directly attributed to the impossibility of this reactant to reach Ti sites inside the channels of Beta zeolite, due to strong diffusional limitations. Moreover, the relatively low activity of cyclohexene on Ti-Beta zeolite, also reported by other authors,^[4] indicates that during epoxidation of cyclohexene, diffusional limitations can also play a role. In fact a decrease in activity for the epoxidation of cycloalkenes with respect to linear alkenes is typically observed with medium pore Ti-zeolites, i.e. TS-1 (5.1 x 5.5 Å, and 5.3 x 5.6 Å) and Ti-MWW (4.0 x 5.5 Å),^[23] owing to diffusional limitations of cycloalkenes into the medium size pores. In the case of Ti-Beta, it is expected that cyclic olefins, such as cyclohexene, will only diffuse through two out of the three channels present in the Beta structure (the two with larger pore diameters, 6.6 x 6.7 Å), while linear alkenes will also diffuse into the third channel with a pore diameter (5.6 x 5.6 Å), that resembles more to the dimensions of the TS-1 medium pore size zeolite. This hypothesis would explain the unusually high ratio 1-hexene/cyclohexene epoxidation observed with Ti-Beta. On the other hand, Ti-BEC, with three large straight pores (7.5 x 6.3 Å and 6.9 x 6.0 Å), is more active than Ti-Beta for the epoxidation of cycloalkenes (Figure 8), with either H₂O₂ or organic peroxides as oxidants. Moreover, the 1-hexene/cyclohexene epoxidation ratio with Ti-BEC is in line from what the chemical reactivity would predict,^[24] indicating that there are not diffusional limitations for cyclohexene within the pores of the Ti-BEC zeolite. The recently discovered Ti-

YNU1,^[5,25] with an effective pore diameter of $\sim 6.5 \text{ \AA}$ gives excellent results for epoxidizing cycloalkenes. Comparative results show that Ti-BEC gives even better results than Ti-YNU-1 for large cycloalkenes, as clearly evidenced from results using cyclooctene as substrate (see Figure 8 and ^[5b]).

The selectivities to epoxides with Ti-Beta and Ti-BEC have been compared at higher conversion levels in Table 7. At similar levels of conversion, both materials present similar selectivity to the desired product in the epoxidation of 1-hexene and cyclooctene. As expected, high yields to cyclooctene epoxide can be obtained with Ti-Beta and Ti-ITQ-17, due to the good stability of the oxirane group.^[24] However, important differences in selectivity were observed when reacting cyclohexene, whose epoxide can be opened much easier.^[24] In this case, a significant higher selectivity to the epoxide occurs with Ti-BEC due to the lower rate of the corresponding diol formed by opening of the epoxide (Table 7), while H_2O_2 efficiency is, in general, good with both zeolites.

We can then conclude that Ti-BEC is more active and selective than Ti-Beta for the epoxidation of more bulky reactants and, more specifically, for C_6 and C_8 cycloalkenes, establishing a new catalytic landmark for Ti containing large pore zeolites.

4.- CONCLUSION

It has been possible to synthesize all silica BEC in absence of K^+ by finding an SDA that matches very well the pores of this structure, maximizing the Van der Waals interactions, between the template and the walls. Molecular calculations have allowed predicting the best SDA among three series of proposed molecular structures. The synthesis of K^+ free pure silica BEC, has allowed the synthesis of the titanosilicate polymorph. This material with straight large pores gives better epoxidation results for larger olefins and, more specifically for cycloalkenes, than Ti-Beta or any of the Ti-large pore zeolites reported up to now.

ACKNOWLEDGMENT. The authors thank the CICYT for financial support (Project MAT 2006-14274-C02-01). G.S. thanks “Centro de Cálculo de la Universidad Politécnica de Valencia” for the use of their computational facilities. M.M. and P.S. thank ITQ for a scholarship.

FIGURES

Figure 1: Organic Structure Directing Agents used in the present work.

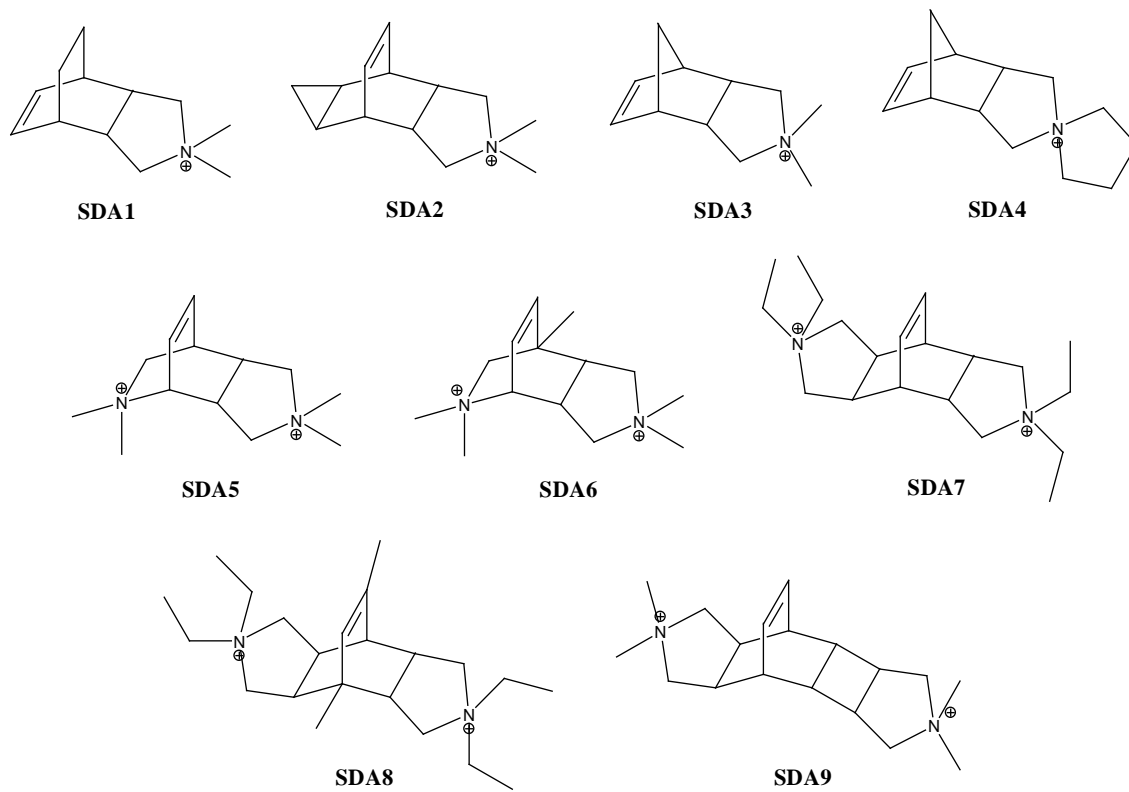


Figure 2: Schematic view of a framework defect in BEC zeolite. A missing Si atom generates leaves four unsaturated O atoms, three of which are saturated by forming terminal SiOH bonds whilst the fourth remains as an unsaturated SiO⁻ bond. The overall charge of the defect is -1.

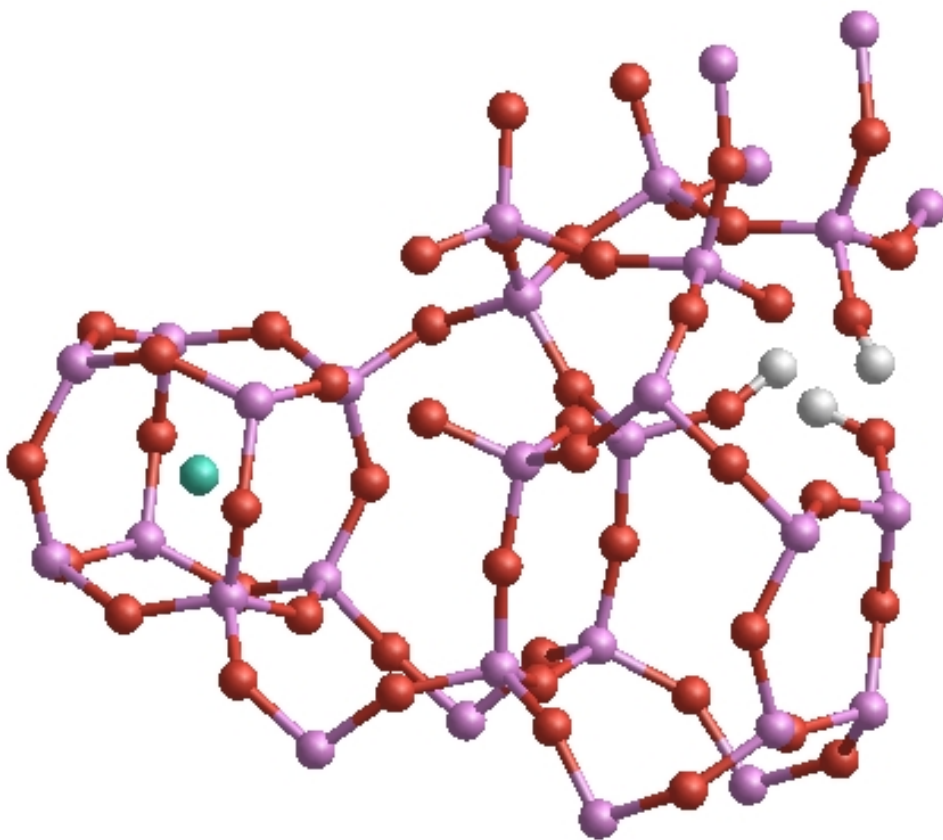


Figure 3: Optimized geometry of SDA9 inside the micropore of pure silica BEC zeolite.

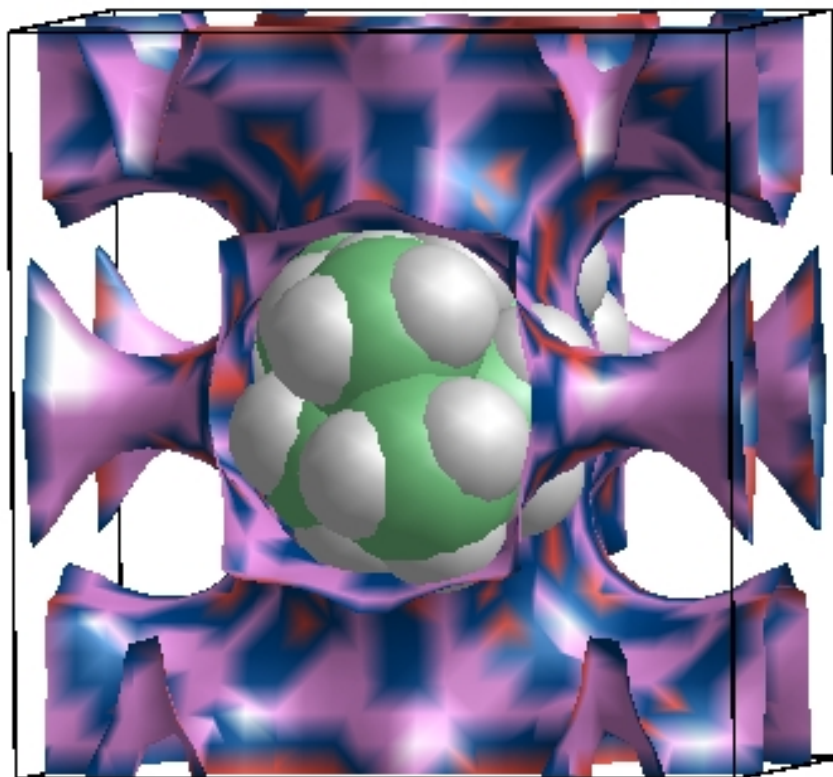


Figure 4: XRD measurements for the as made and calcined ITQ-17 zeolite synthesized using SDA9 as SDA.

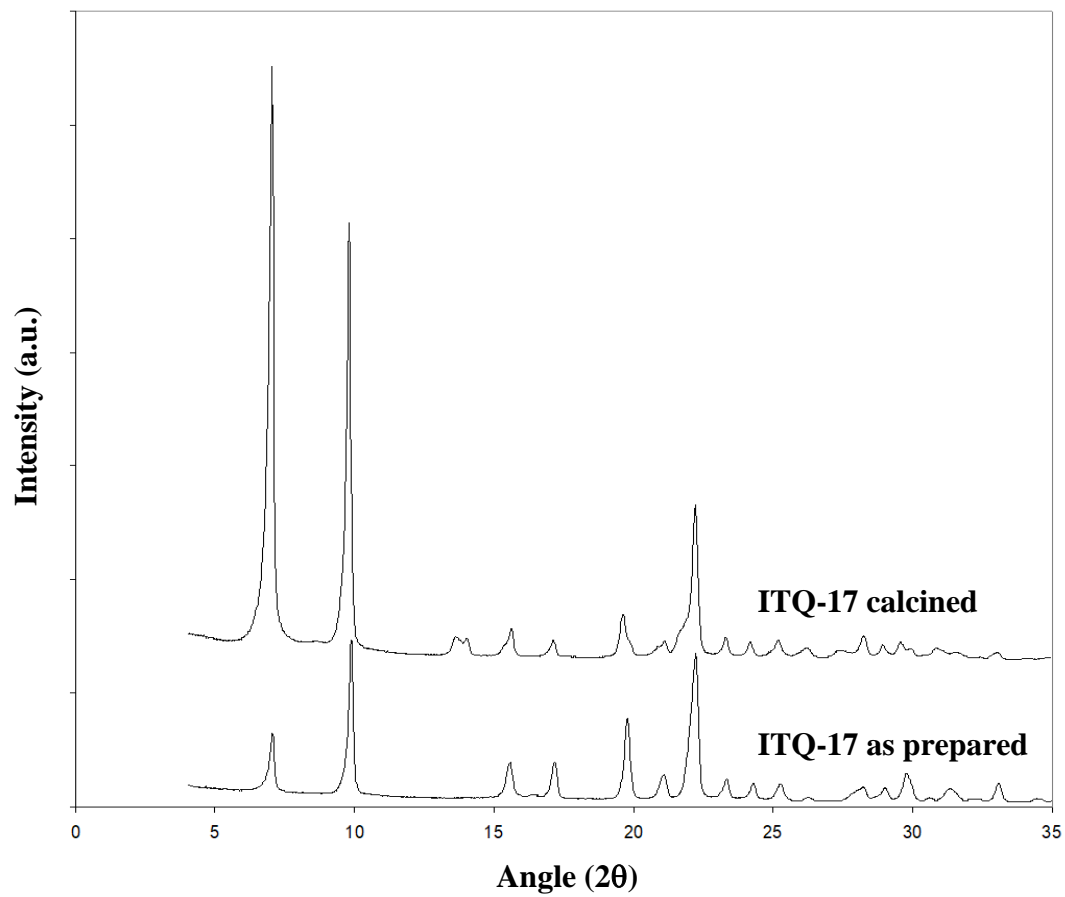


Figure 5: ^{19}F MAS NMR spectra of the as made ITQ-17 zeolite synthesized using SDA9 as SDA.

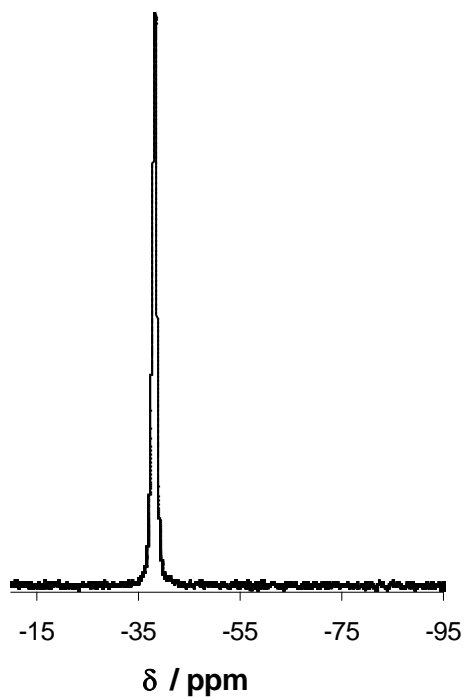


Figure 6: ^{29}Si MAS NMR spectra of the calcined pure silica ITQ-17 samples.

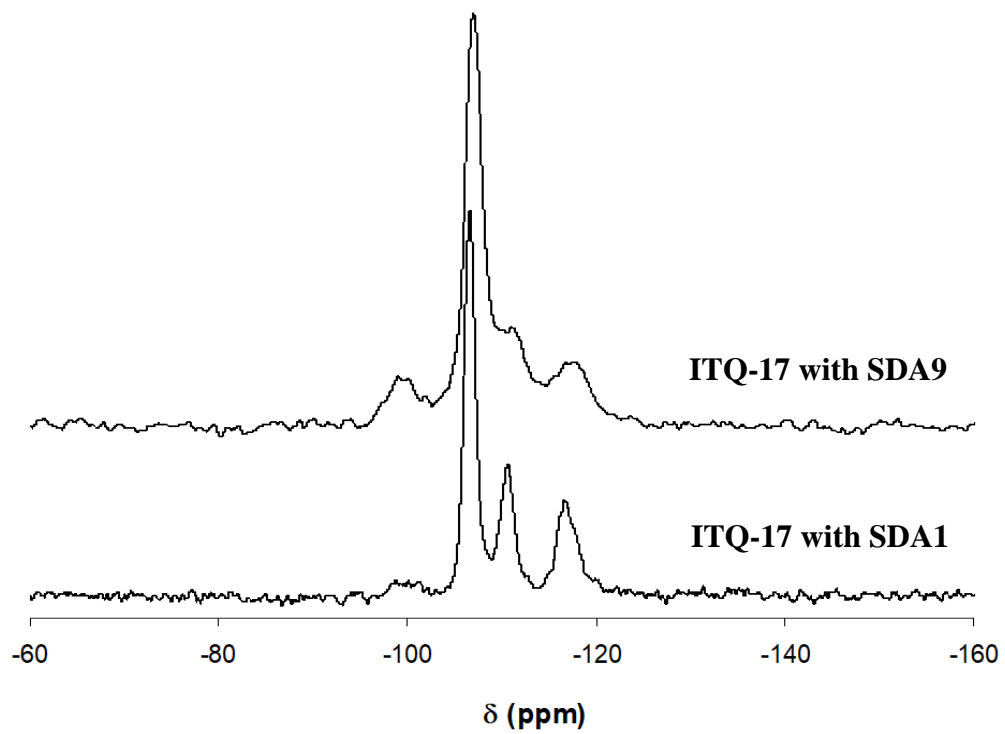


Figure 7: UV-vis DRS spectra of Ti-microporous materials.

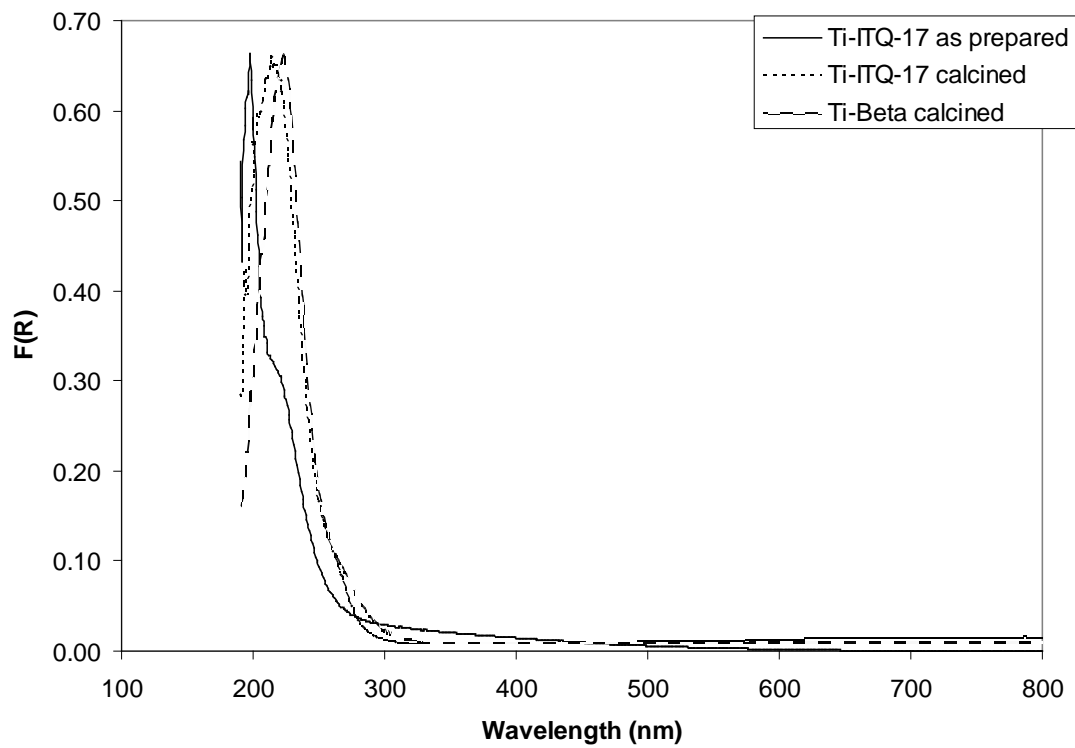
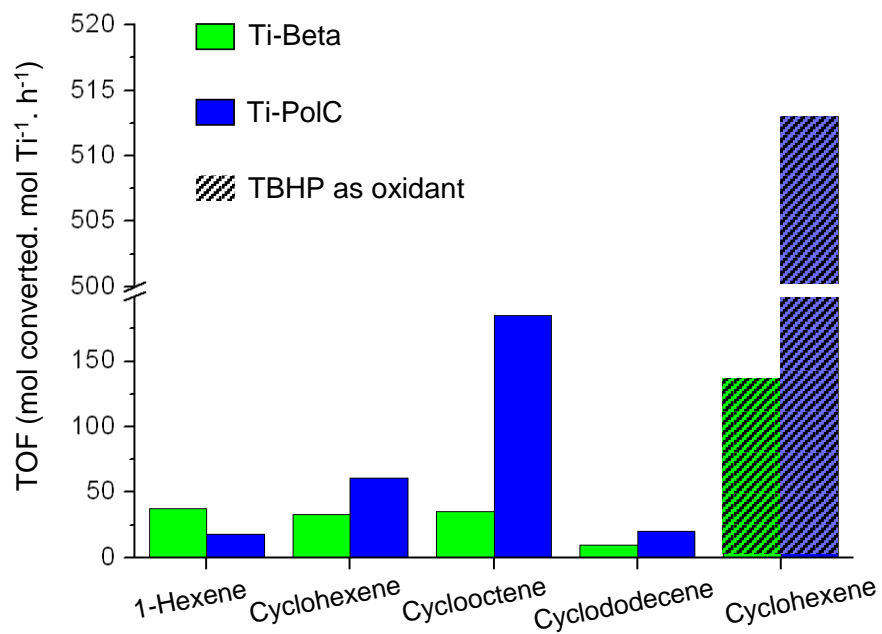


Figure 8: Intrinsic activity of Ti-Beta and Ti-ITQ-17, expressed as turnover frequency number (mmol alkene converted/mmol Ti.h), on the epoxidation of different substrates with H₂O₂.



TABLES.

Table 1: Calculated energy terms to form the system pure silica BEC-SDA (monocationic SDA) from the components as defined in equation 1. The different SDAs are shown in Figure 1. The energies shown correspond to the unit cell considered in the calculations ($32\text{SiO}_2 + 2 \text{SDA}^+ + 2 \text{F}^-$).

SDA	$E^{\text{vdW}}_{\text{zeo-SDA}}^{(a)}$ (eV)	$E^{\text{coul}}_{\text{SDA,F}}^{(b)}$ (eV)	$\Delta E_{\text{SDA}}^{(c)}$ (eV)	$E^{(d)}$ (eV)
SDA1	-2.36	-6.40	0.11	-8.65
SDA2	-2.40	-6.34	0.21	-8.53
SDA3	-2.16	-6.35	0.10	-8.41
SDA4	-2.46	-6.24	0.09	-8.61

^a Energy of the short-range intermolecular interactions between all the SDA molecules in the unit cell and the zeolite structure.

^b Electrostatic energy of the ions (the SDA has +1 charge and the fluorine has -1 charge). This electrostatic term is a summation over the following terms: $\text{SDA}^+-\text{SDA}^+$, F^--F^- , and SDA^+-F^- . The coulombic intra-SDA energy should not be taken into account as this does not contribute to the effect of stability and hence it is not included in the summation, where only intermolecular terms are counted.

^c Total strain energy deformation of the SDA molecules in the unit cell with respect to the ground state divided by the number of SDA molecules. This gives an average of the stress energy per SDA molecule inside the micropore of pure silica BEC.

^d Energy resulting from the summation of the first three contributions.

Table 2: Calculated energy terms to form the system pure silica BEC-SDA (dicationic SDA) from the components as defined in equation 1. The SDAs are shown in Figure 1. Results of SDA8 are not shown because it is not a stable molecule inside the BEC micropore.

SDA	$E_{\text{zeO-SDA}}^{\text{vdW}}$ ^(a) (eV)	ΔE_{SDA} ^(b) (eV)
SDA5	-2.56	0.20
SDA6	-2.40	0.31
SDA7	-2.30	0.42
SDA9	-3.32	0.22

^a Energy of the short-range intermolecular interactions between all the SDA molecules in the unit cell and the zeolite structure.

^b Total strain energy deformation of the SDA molecules in the unit cell with respect to the ground state divided by the number of SDA molecules. This gives an average of the stress energy per SDA molecule inside the micropore of pure silica BEC.

Table 3: Calculated relative energy of the system pure silica BEC-SDA (dicationic SDA) in the presence of fluoride and framework-defect anions. The energies shown correspond to the unit cell considered in the calculations whose stoichiometry corresponds to: $30\text{SiO}_2 + 2\text{H}_2\text{O} + 2\text{OH}^- + 2\text{F}^- + 2\text{SDA}^{2+}$. Defects can be formed in different parts of the structure and hence not only one but five defect configurations have been considered.

Defect-config.	SDA5 ^(a) (eV)	SDA6 (eV)	SDA7 (eV)	SDA9 (eV)
config-1	2.82	1.46	1.70	1.52
config-2	0.32	1.23	1.16	0.99
config-3	1.88	1.75	2.10	0.66
config-4	0.00	0.82	1.22	0.85
config-5	1.42	0.77	2.05	0.78
Average ^(b)	1.29	1.21	1.65	0.96

^a Total energy excluding the SDA-stress. The system optimised contains: (i) a BEC silica framework with 2 defects (each being formed by three terminal SiOH groups and one unsaturated SiO[•] bond); (ii) 2 SDA²⁺ molecules (SDA5, SDA6, SDA7, SDA9); (iii) and 2 F⁻ anions. The electrostatic contribution to this energy is a summation over the following terms: defect-SDA⁺, defect-F⁻, defect-defect, SDA⁺-SDA⁺, F⁻-F⁻, and SDA⁺-F⁻. The SDA-stress energies are included in Table 1.

^b Average total energy of the BEC-SDA²⁺-F⁻ considering the presence of structural defects on the BEC framework as experimentally detected. The total energy excludes the SDA-stress energy whose value is in Table 2.

Table 4: Pure silica phases formed using SDAs of Figure 1 without alkali cations.

SDA	Phase formed
SDA1	Beta
SDA2	Beta
SDA3	Beta
SDA4	Beta
SDA5	Amorphous
SDA6	Amorphous
SDA7	Beta
SDA8	ITQ-24
SDA9	ITQ-17

Table 5: Pure silica ITQ-17 with different SDAs.

SDA	N	C	H	SDA/u.c
SDA1	1.39	17.77	2.18	2.5
SDA9	2.11	16.90	2.11	1.9

Table 6: Ti content in ITQ-17.

Theoretical content (%wt TiO₂/SiO₂)	Real content (%wt TiO₂/SiO₂)
2	0.55

Table 7: Cyclohexene and 1-Hexene epoxidation over Ti-Beta and Ti-ITQ-17.

Substrate	Catalyst	Si/Ti	Time (min)	Conv. (% of Maximum)	% S Epoxide	% S Diol^a	% S H₂O₂	% S TBHP
1-Hexene	Ti-Beta	59	45	20,1	97,0	2,6	89,9	---
1-Hexene	Ti-PolC	240	120	13	97,1	2,2	40,3	---
Cyclohexene	Ti-Beta	59	90	31,2	57,8	28,6	81,8	---
Cyclohexene	Ti-PolC	240	90	25,4	70,4	20,2	89,7	---
Cyclohexene ^b	Ti-Beta	59	325	40,8	72,4	16,8	---	90,4
Cyclohexene ^b	Ti-PolC	240	135	43,9	83,7	10,5	---	93,8
Cyclooctene	Ti-Beta	59	90	44,2	98,1	1,7	87,3	---
Cyclooctene	Ti-PolC	240	90	69,8	98,5	1,4	96,5	---

^a Other by-products consisting on 2-cyclohexene-1-ol, and 2-cyclohexene1-one.

^b Experiment using TBHP as oxidant agent under solvent-free conditions

SUPPLEMENTARY MATERIAL

In a first approximation for the dications SDA5-SDA9, a way to obtain a neutral system is to average the SDA charge to +1 by a procedure already used in previous studies.ⁱ Whilst this is a certain shortcoming in the calculations, it represents a reasonably accurate way of simulating a neutral system. For our current purpose here we are only interested in getting a good approximation to the short range van der Waals energy and the SDA stress energy, and both energetic terms are quite independent of the electrostatics of the system. Strictly speaking only the fact that the full system is energy minimised makes the energetic results dependent of the electrostatics but once the system has been optimised, the mentioned energetic terms are totally independent of the charge distribution and hence this approach is very reasonable to calculate van der Waals and stress terms.

In this approximation we calculate two contributions: the short-range (van der Waals) interaction zeolite-SDA ($E_{\text{zeo-SDA}}^{\text{vdW}}$), and the SDA strain (ΔE_{SDA}) whose results are shown in Table 2. It can be seen that SDA9 is the most favorable due to its very low short range contribution which indicates a very high template effect due to an excellent matching between the shape of SDA9 and the BEC micropore. The SDA9 is not highly stressed in its optimised conformation as shown in Table 2 by the relatively low value of ΔE_{SDA} , and this also points to its good capability as SDA in pure silica BEC zeolite. On the other hand, SDA7 looks very unfavorable due to high strain energy of this SDA inside the micropore, and the same happens for SDA8 which could not even be optimized in the micropore due to a clear too large size of this molecule.

(i) (a) Sastre, G.; Lewis, D. W.; Catlow, C. R. A. *J. Phys. Chem.* **1996**, *100*, 6722. (b) Sastre, G.; Fornes, V.; Corma, A. *J. Phys. Chem. B.* **2002**, *106*, 701.

REFERENCES

- (1) Corma, A. *Catal. Rev. Sci. Eng.* **2004**, *46*, 369.
- (2) (a) Millini, R.; Massara, E. P.; Perego, G.; Bellussi, G. *J. Catal.* **1992**, *137*, 497. (b) Ingallina, P.; Clerici, M. G.; Rossi, L.; Bellussi, G. *Stud. Surf. Sci. Catal.* **1995**, *92*, 31. (c) Thangaraj, A.; Kumar, R.; Ratnasamy, P. *J. Catal.* **1991**, *131*, 294. (d) Corma, A.; Nemeth, L.; Renz, M.; Valencia, S. *Nature*. **2001**, *412*, 423. (e) Renz, M.; Blasco, T.; Corma, A.; Fornes, V.; Jensen, R.; Nemeth, L. *Chem. Eur. J.* **2002**, *8*, 4708. (f) Notestein, J. M.; Katz, A. *Chem. Eur. J.* **2006**, *12*, 3954. (g) Wu, P.; Liu, Y.; He, M.; Tatsumi, T. *J. Catal.* **2004**, *228*, 183.
- (3) Tamarasso, M.; Perego, G.; Notari, B. *U.S. Patent 4.4410.501*, **1983**.
- (4) (a) Cambor, M.A.; Costantini, M.; Corma, A.; Gilbert, L.; Esteve, P.; Martínez, A.; Valencia, S. *Chem. Commun.* **1996**, 1339. (b) Van der Waal, J. C.; Rigutto, M. S.; Van Bekkum, H. *Appl. Catal. A.* **1998**, *167*, 331.
- (5) (a) Fan, W.; Wu, P.; Namba, S.; Tatsumi, T. *Angew. Chem., Int. Ed.* **2003**, *43*, 236. (b) Fan, W.; Wu, P.; Namba, S.; Tatsumi, T. *J. Catal.* **2006**, *243*, 183.
- (6) Treacy, M. M. J.; Newsam, J. M. *Nature*. **1988**, *332*, 249.
- (7) Conradsson, T.; Dadachov, M. S.; Zou, X. D. *Micropor. Mesopor. Mat.* **2000**, *41*, 183.
- (8) Corma, A.; Navarro, M. T.; Rey, F.; Rius, J.; Valencia, S. *Angew. Chem., Int. Ed.* **2001**, *40*, 2277.
- (9) Cantín, A.; Corma, A.; Díaz-Cabañas, M. J.; Jordá, J. L.; Moliner, M.; Rey, F. *Angew. Chem., Int. Ed.* **2006**, *45*, 8013.
- (10) Cambor, M. A.; Corma, A.; Perez-Pariente, J. *Zeolites*. **1993**, *13*, 82.

-
- (11) Computer Simulation of Solids, Eds. Catlow, C. R. A.; Mackrodt, W. C.; Lecture Notes in Physics, Vol. 166, Springer, Berlin, **1982**
- (12) (a) Catlow, C. R. A.; Cormack, A. N. *Int. Rev. Phys. Chem.* **1987**, *6*, 227. (b) Schroder, K.-P.; Sauer, J.; Leslie, M.; Catlow, C. R. A.; Thomas, J. M. *Chem. Phys. Lett.* **1992**, *188*, 320.
- (13) (a) Gale, J. D. *J. Chem. Soc. Faraday Trans.* **1997**, *93*, 629. (b) Gale, J. D.; Rohl, A. L.; *Mol. Simul.* **2003**, *29*, 291.
- (14) Sastre, G.; Gale, J. D. *Chem. Mater.* **2003**, *15*, 1788.
- (15) Sastre, G.; Gale, J. D. *Chem. Mater.*, **2005**, *17*, 730.
- (16) Kiselev, A. V.; Lopatkin, A. A.; Shulga, A. A. *Zeolites*. **1985**, *5*, 261.
- (17) Oie, T.; Maggiora, T. M.; Christoffersen, R. E.; Duchamp, D. J. *Int. J. Quantum Chem., Quantum Biol. Symp.* **1981**, *8*, 1.
- (18) Rappe, A. K. ; Goddard, W. A. *J. Phys. Chem.* **1991**, *95*, 3358.
- (19) (a) Sastre, G.; Leiva, S.; Sabater, M. J.; Gimenez, I.; Rey, F.; Valencia, S.; Corma, A. *J. Phys. Chem. B.* **2003**, *107*, 5432. (b) Sastre, G. ; Cantin, A.; Diaz-Cabañas, M. J. ; Corma, A. *Chem. Mater.* **2005**, *17*, 545.
- (20) Coffen, D. L. ; Hengartner, U.; Katonak, D. A.; Mulligan, M. E.; Burdick, D. C.; Olson, G. L.; Todaro, L. J. *J. Org. Chem.* **1984**, *49*, 5109
- (21) Schroder, K.-P., Sauer, J.; Leslie, M.; Catlow, C. R. A.; Thomas, J. M. *Chem. Phys. Lett.* **1992**, *188*, 320.
- (22) Zecchina, A.; Spoto, G.; Bordiga, S.; Ferrero, A.; Petrini, G.; Leofanti, G.; Padovan; M. *Stud. Surf. Sci. Catal.* **1991**, *69*, 251.

(23) Baerlocher, Ch.; Meier, W. M.; Olson, D. H. *Atlas of Zeolite Framework Types*, Elsevier, Amsterdam, **2001**.

(24) Arends, I. W. C. E.; Sheldon, R. E. *Topics in Catalysis*. **2002**, *19*, 133.

(25) Ruan, J.; Wu, P.; Slater, B.; Terasaki, O. *Angew. Chem., Int. Ed.* **2005**, *44*, 6719.